ELSEVIER

Journal of Structural Geology 27 (2005) 943–947

JOURNAL OF STRUCTURAL GEOLOGY

www.elsevier.com/locate/jsg

Brittle deformation of quartz in a diamond anvil cell

J. Bisschop[a,*], B. den Brok[a], R. Miletich[b]

[a]*Geologisches Institut, ETH-Zürich, CH-8092, Switzerland*
[b]*Mineralogisches Institut, University of Heidelberg, D-69120, Germany*

Received 6 October 2004; received in revised form 21 March 2005; accepted 21 March 2005
Available online 13 June 2005

Abstract

Quartz single crystals were deformed by brittle processes in a diamond anvil cell at high confining pressure (800–1200 MPa) and room temperature in the presence of water.

Keywords: Quartz; Diamond anvil cell; Deformation; Microcracking

1. Introduction

We investigated if quartz can be deformed in a diamond anvil cell (DAC) under an optical microscope with the aim of making in situ observations of quartz deformation processes at high pressure and temperature and in the presence of water. Although the DAC is designed for experiments under high *hydrostatic* pressure conditions, it is possible—in principle—to stress samples *non-hydrostatically* by 'squeezing' them between the diamond anvils (conf. e.g. Chai and Brown, 1996; Merkel et al., 2003). In this paper we show *how* to control the sample deformation and confining pressure in a DAC in room temperature experiments. First, observations of brittle deformation processes of quartz at high confining (water) pressure are presented. To enter the ductile deformation regime of quartz, experiments need to be carried out in the hydrothermal-DAC in which temperatures up to 1200 °C can be reached (Bassett et al., 1993).

2. Method

The DAC we used was made at ETH in Zürich (Miletich et al., 2000) and consists of an upper and a lower module that are brought together by manual tightening of four screws (Fig. 1a). The anvils are aligned using a rotational hemisphere in the upper module and a translation stage in the lower module. The seats were made of hardened silver steel in which a conical optical access-hole was drilled with a numerical aperture of 0.35. Such an aperture has the resolving power of a 20× long-working-distance objective. We used cone-cut anvils made of gem grade moissanite SiC (from Charles and Colvard, Ltd) instead of much more expensive diamond (conf. Xu et al., 2002). Good in situ optical quality images can be obtained in both *natural* and *polarized* light as long as the crystallographic orientation of the upper anvil is chosen correctly (the *c*-axis of moissanite should be perpendicular to the anvil axis). The culet face of the anvils we used was 1.2 mm in diameter, allowing for a 600 μm diameter pressure chamber.

The pressure chamber was created by placing a 200-μm-thick gasket (with a 600 μm diameter central hole) between the anvil culet faces. The gaskets were made of a soft type of stainless steel (Aisi 304 steel, #4301). Distilled water was used as the pressure medium. The samples were rectangular fragments selected from crushed plates of natural Brazilian quartz single-crystals. The plates were polished (finished with 0.25 μm diamond paste) to a thickness in the range 115–130 μm with plane and parallel surfaces. The water pressure was measured in situ with the ruby fluorescence

* Corresponding author. Address: Center for Physics of Geological Processes, Department of Physics, University of Oslo, P.O. Box 1048, Blindern, 0316 Oslo, Norway. Tel.: +47 22 85 64 85; fax: +47 22 85 51 01

E-mail address: jan.bisschop@fys.uio.no (J. Bisschop).

0191-8141/$ - see front matter © 2005 Elsevier Ltd. All rights reserved.
doi:10.1016/j.jsg.2005.03.001

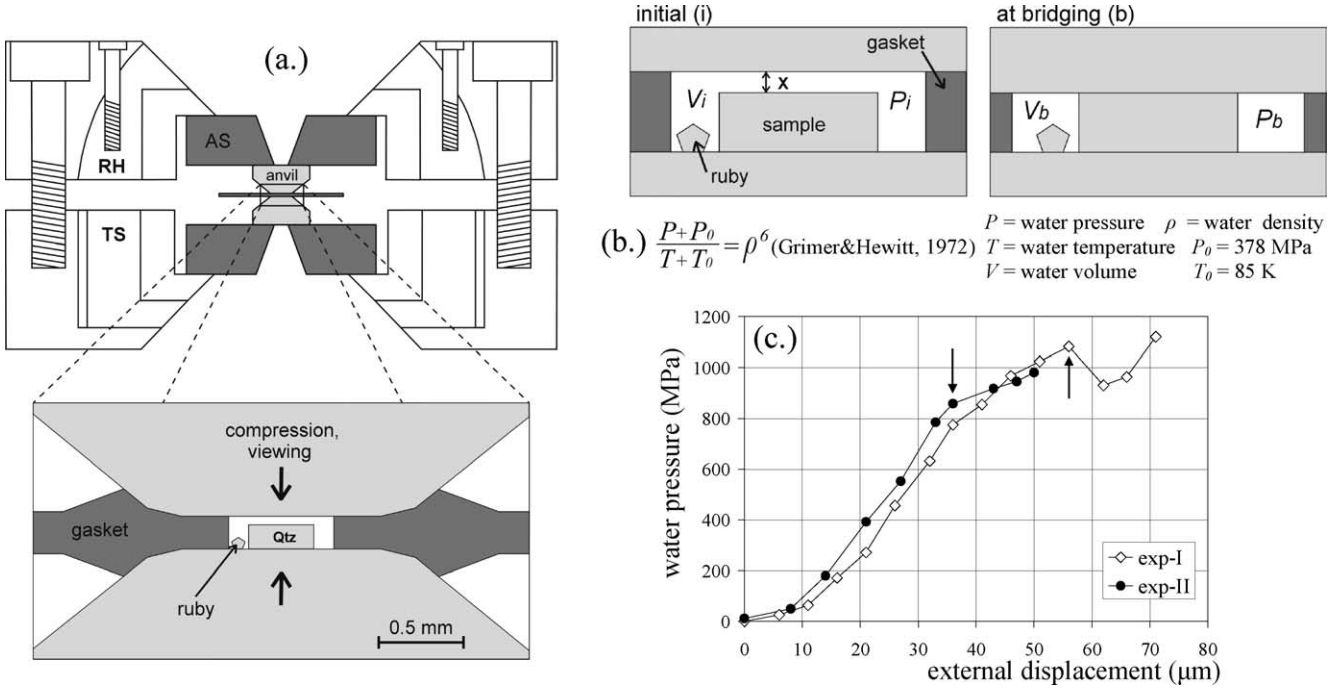

Fig. 1. (a) Cross-section view of the ETH diamond anvil cell (Miletich et al., 2000) with rotational hemisphere (RH), translation stage (TS), and anvil seats (AS). Lower image shows pressure chamber (to scale) with the quartz sample and ruby pressure calibrant (the upper anvil is drawn in a position where it does not touch the sample). (b) Principle of sample deformation and control of confining pressure in the DAC. When sample bridges both anvils, *hydrostatic* compression of the sample changes into *non-hydrostatic* deformation of the sample. Initial height difference between sample and chamber (X) will determine the water pressure at bridging (P_b). The empirical relationship of water pressure and density (Grimer and Hewitt, 1972) was used to calculate X for a P_b of 1 GPa. (c) Water pressure versus external displacement in experiments I and II. Arrows indicate the moments of sample bridging. In experiment II a moissanite anvil failed upon tightening the screws above 50 μm.

method (Barnett et al., 1973), requiring a small ruby crystal to be placed in the pressure chamber in each experiment.

On tightening the screws, the anvils intrude the gasket and water pressure builds-up. In the beginning, the upper anvil does not touch the sample (Fig. 1b); the stress state in the sample is hydrostatic during this stage. The 'bridging pressure' is the water pressure at the moment that the upper anvil touches the sample—this is the confining pressure at the moment when the deformation of the sample starts. The initial chamber height and diameter required to arrive at a specific bridging pressure (~1 GPa in our experiments) was calculated in advance—taking into account the height and volume of the sample and the volume of the ruby crystal—using the empirical relationship between pressure and density of water at high pressure (Fig. 1b). The initial chamber height was controlled by pre-indenting the gasket. The only unknown parameter in the calculation was the chamber *diameter* at the moment of sample bridging, but this parameter was estimated from observations made in previous experiments. In our experiments the actual, measured bridging pressure was within 200 MPa of the calculated bridging pressure.

We were not able to measure the anvil displacement accurately during the experiments. Instead, the displacement of the upper and lower modules were measured, externally, with a micrometer on the four sides of the DAC. The average of these four measurements is what we refer to as 'external displacement' in this paper. The modules were advanced in steps of 5–10 μm by manual tightening of the four screws. In order to make the anvils advance without loss of anvil alignment, screws (with opposite threads) in opposite corners were tightened simultaneously in tiny steps. Immediately (approximately 1 min) after reaching the required external displacement, in situ images of the sample were taken with a digital camera (Nikon DN 100) on a transmitted-light microscope (Nikon Eclipse E 600) with a 20× super-long-working-distance objective (LU Plan WD 24). The water pressure was measured immediately after (time-dependent) cracking in the sample appeared to have stopped. With the ruby fluorescence method, water pressures could be measured with a precision of 50 MPa (Barnett et al., 1973). In our experiments the average value of nine measurements per loading step had a standard deviation of generally less than 10 MPa.

We present the results of three successful experiments carried out at room temperature: experiments I and II were carried out 'undrained', i.e. under *high* water pressure, and experiment III was carried out 'drained', i.e. under *low*, atmospheric water pressure. To make sure that water pressure remained atmospheric in experiment III, a thin scratch was made on the upper side of the gasket so that the chamber would leak. An air bubble was present in the chamber during the entire experiment III, indicating that water pressure had indeed been atmospheric.

3. Results

The water pressure as a function of external displacement of the DAC in experiments I and II is shown in Fig. 1c. The moment the anvils touch the sample can be observed in situ by the appearance of interference 'Newton' fringes caused by the extremely thin water wedge present between the sample and the anvil just before they touch. As soon as the anvils make full contact with the sample (as in Fig. 2a) these fringes disappear. Moreover, small dirt particles on the sample surface are visibly squeezed when the upper anvil touches the sample. In experiment I the water pressure dropped by 150 MPa soon after bridging, possibly due to water leakage.

Fig. 2 shows in situ images of brittle fragmentation of the samples in experiment I and II during progressive loading. In both experiments, small flakes broke off from the sample sides and fine branching cracks gradually propagated into the sample. In experiment II, a fine network of cracks developed in one corner of the sample only. In both experiments cracks grew instantaneously after having increased the stress. At higher degrees of external displacement, time-dependent crack-growth was observed. Some cracks and crack-branches in experiment II seem to show a preferred propagation direction (arrow in Fig. 2k).

Brittle sample deformation at atmospheric confining pressure was distinctively different from that observed at high confining pressure. The entire sample was crushed instantaneously at a critical load. Before this macroscopic yielding, two or three long cracks developed gradually upon tightening the screws (Fig. 3). At the start of deformation, a number of short cracks appeared in the sample centre that did not develop any further in time or upon tightening of the screws.

4. Discussion

Water pressure could have affected sample fragmentation in the DAC in two ways: first, the room temperature failure strength of quartz (compressed parallel to the *c*-axis) is ~3 GPa at atmospheric pressure and 5.3 at 0.5 GPa confining pressure (Griggs et al., 1960). Thus, in experiments I and II, the water-confined samples were able to sustain larger stresses than the sample in experiment III. Second, water pressure might affect sample–anvil friction

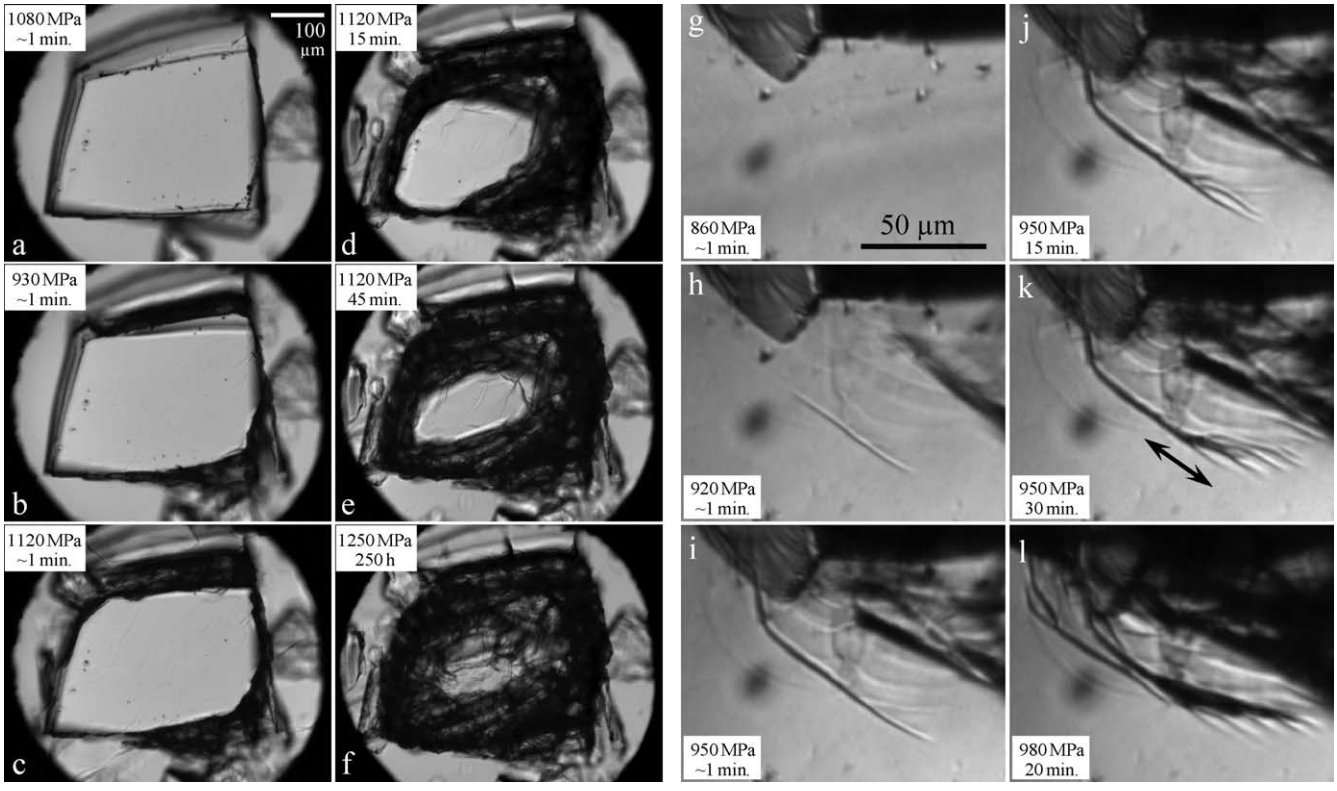

Fig. 2. In situ optical micrographs of quartz samples deformed at high water pressure in the DAC in experiments I ((a)–(f)) and II ((g)–(l)). Water pressure and the time at which the images were taken *after* renewed tightening of the screws (i.e. increasing the load) are indicated in each image. (a)–(f) Experiment I: initial chamber diameter 570 µm; sample thickness 124 µm; quartz *c*-axis oriented parallel to the compression direction. (g)–(l) Detail of a corner of quartz sample deformed in experiment II: sample thickness is 118 µm; quartz *c*-axis oriented perpendicular to the compression direction (*c*-axis direction in plane of paper not known). Parts (b) and (c) from experiment I and (h) and (i) from experiment II show the instantaneous crack-growth that occurred upon tightening the screws. Parts (d)–(f) from experiment I and (j) and (k) from experiment II show time-dependent cracking at constant external displacement. A micrograph (f) was taken at the same external displacement as (e) but water pressure increased for unclear reasons from 1120 to 1250 MPa in 250 h. The finite axial sample shortening in experiment I measured ex situ after the experiment from the intruded gasket was 12 ± 1 µm (=10% strain).

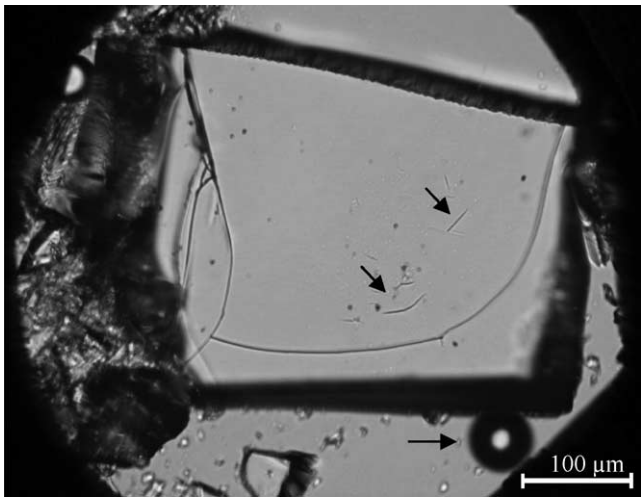

Fig. 3. In situ optical micrograph of cracks in the quartz sample deformed at atmospheric water pressure in the DAC in experiment III. Sample thickness is 126 μm; quartz *c*-axis oriented parallel to compression direction. Further screw-tightening by 5 μm after this image was taken resulted in complete crushing of the sample. Arrows show short cracks in the core of the sample and an air bubble. The image was taken with strongly reduced condenser diaphragm to increase the depth of focus.

and thus affect the stress distribution in the sample. Possibly the presence of (trapped) thin water films at the sample–anvil contacts in the high water pressure experiments I and II reduced the friction. At atmospheric pressure (experiment III) water may be squeezed out more easily between the anvil and the sample.

Chai and Brown (1996) showed that the stress distribution in samples differentially stressed in a DAC depends on the amount of friction. If friction is low (as possibly in experiments I and II) stresses are uniformly distributed through the sample; if friction is high (as possibly in experiment III) stresses are heterogeneously distributed and the highest pressure is attained in the sample centre. For this reason, crack initiation may have been easier at sample *edges* in experiments I and II, and in the sample *centre* in experiment III. In experiments I and II, the high confining pressure did not suppress crack-propagation since the sample was not jacketed and the confining medium penetrated the cracks.

Undulating groove-like features developed on the upper surface of the sample in experiment I (Fig. 4). They had a depth of less than a few μm. A rose diagram (inset in Fig. 4) shows that the grooves comprise a partially oriented system with a preferred NE–SW direction. The grooves developed from the moment of sample bridging and remained where they were, i.e. did not move like the grooves observed on stressed mineral faces by den Brok et al. (2002). It is not known how these grooves formed. Possibly, they are due to crystal-plastic deformation induced by (trapped) water squeezed out from the sample–anvil interface in a channel-like fashion at high stress and water pressure. Plastic deformation of quartz at room temperature is known from Vickers indentation tests (e.g. Masuda et al., 2000). Further experiments are required to elucidate the mechanical and possibly chemical explanation for these grooves.

Acknowledgements

This project was financed by the Netherlands Organization for Scientific Research (NWO, Grant No. S77-184) and the Swiss Federal Institute of Technology (ETH) in Zürich. The technical assistance of Gunter Krauss, Hans Reifler, Robert Hofmann, Marcel Mettler and Frowin Pirovino in the project was strongly appreciated.

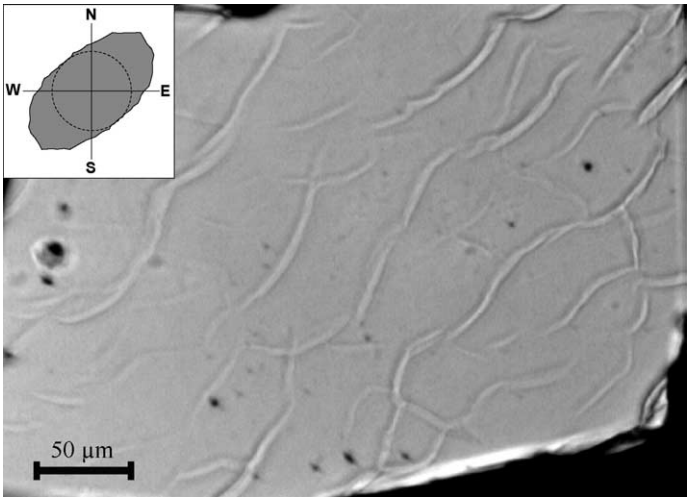

Fig. 4. In situ optical micrograph of groove-like surface structures that developed on the upper surface of the sample in experiment I. In this experiment the quartz *c*-axis was parallel to the compression direction. The image was taken at 950 MPa water pressure. To highlight the surface features, the microscope condenser diaphragm was reduced and the contrast of the digital image enhanced. Inset shows a rose diagram of the overall orientation of the grooves. The diagram gives the reciprocal value of the number of intersections of the traced groove pattern with a test grid of parallel lines ($\Delta = 8$ μm) rotated in steps of 5 ° (see Underwood, 1970).

References

Barnett, J.D., Block, S., Piermarini, G.J., 1973. An optical fluorescence system for quantitative pressure measurement in the diamond-anvil cell. Review of Scientific Instruments 44, 1–9.

Bassett, W.A., Shen, A.H., Bucknum, Chou, I.-M., 1993. A new diamond anvil cell for hydrothermal studies to 2.5 GPa and from −190 to 1200 °C. Review of Scientific Instruments 64 (8), 2340–2345.

Chai, M., Brown, J.M., 1996. Effect of static non-hydrostatic stress on the R lines of ruby single crystals. Geophysical Research Letters 23 (24), 3539–3542.

den Brok, S.W.J., Zahid, M., Morel, J., 2002. In situ experimental study of roughness development at a stressed solid/fluid interface. In: de Meer, S., Drury, M.R., de Bresser, J.H.P., Pennock, G.M. (Eds.), Deformation Mechanisms, Rheology and Tectonics: Current Status and Future Perspectives Geological Society, London, Special Publications, 200, pp. 73–83.

Griggs, D.T., Turner, F.J., Heard, H.C., 1960. Deformation of rocks at 500 and 800 °C. Geological Society of America Memoirs 79, 39–104.

Grimer, F.J., Hewitt, R.E., 1969. The form of the stress–strain curve of concrete interpreted with a di-phase concept of material behaviour. In: Te'eni, M. (Ed.), Structure, Solid Mechanics and Engineering Design Proceedings of the Southampton 1969 Civil Engineering Conference. Wiley, New York, pp. 681–691 (see also: http://www.sbu.ac.uk/water/strange.html).

Masuda, T., Hiraga, T., Ikei, H., Kanda, H., Kugimiya, Y., Akizuki, M., 2000. Plastic deformation of quartz at room temperature: a Vickers nano-indentation test. Geophysical Research Letters 27 (17), 2773–2776.

Merkel, S., Wenk, H.R., Badro, J., Montagnac, G., Gillet, P., Mao, H-K., Hemley, R.J., 2003. Deformation of (Mg0.9Fe0.1)SiO3 Perovskite aggregates up to 32 GPa. Earth and Planetary Science Letters 209, 351–360.

Miletich, R., Allan, D.R., Kuhs, W.F., 2000. High-pressure single-crystal techniques. In: Hazen, R.M., Downs, R.T. (Eds.), Reviews in Mineralogy and Geochemistry 41. High-Temperature and High-Pressure Crystal Chemistry, pp. 445–519.

Underwood, E.E., 1970. Quantitative Stereology. Addison-Wesley, 48–58.

Xu, J.-A., Mao, H-K., Hemley, R.J., Hines, E., 2002. The moissanite anvil cell: a new tool for high-pressure research. Journal of Physics: Condensed Matter 14, 11543–11548.